Multimodal optical spectrometers for remote chemical detection.

E.C. Cull, M.E. Gehm, S.T. McCain, B.D. Guenther, and D.J. Brady

Duke University Fitzpatrick Center for Photonics and Communications Systems, Durham, NC 27708

ABSTRACT

We have developed a class of aperture coding schemes for Remote Raman Spectrometers (RRS) that remove the traditional trade-off between throughput and spectral resolution. As a result, the size of the remote interrogation region can be driven by operational, rather than optical considerations. We present theoretical arguments on the performance of these codes and present data from where we have utilized these codes in other spectroscopy efforts.

Keywords: Remote sensing, Raman spectroscopy, LIDAR, multiplex measurement

1. INTRODUCTION

Recent world events have greatly increased the need for systems capable of remote chemical detection.[1] Currently, a leading mechanism for effecting such detection is Remote Raman Spectroscopy (RRS). In this modality, excitation laser light is projected onto the target of interest and Raman scattered light is collected by a telescope and coupled into a spectrometer. A schematic of this type of system is shown in Fig. 1. The spectrum of the Raman scattered light contains features which can be used to uniquely identify trace chemical compounds on the target. The light becomes an "optical fingerprint" of the chemical environment at the target.

The interrogation region acts as an incoherent source of Raman photons. The emission has a broad (nominally isotropic) angular profile, and the spatial extent is the size of the excitation source. When working with incoherent sources, traditional spectrometers have an inherent trade-off between throughput and spectral resolution as a result of the spatial-filtering provided by the input slit of the spectrometer. In RRS, however, the collected light is already spatially-filtered to a significant degree by the fact that the telescope subtends only a small solid angle as seen from the target. This "prefiltering" improves the situation somewhat, but ultimately, a traditional spectrometer must either be light starved, or have low resolution.

Further author information: Send correspondence to dbrady@duke.edu

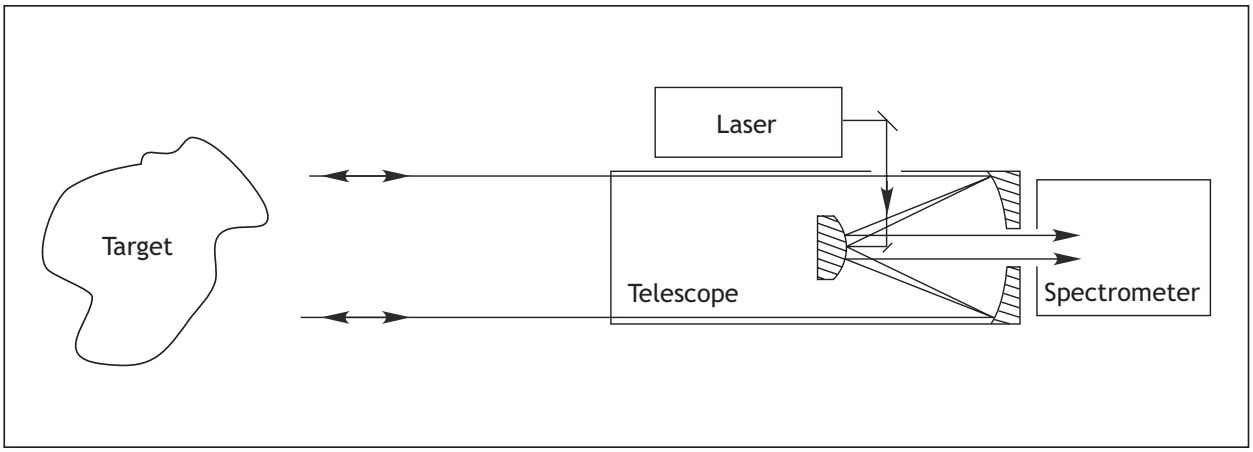

Figure 1. Typical optical system schematic for an RRS.

Sensors, and C3I Technologies for Homeland Security and Homeland Defense IV, edited by Edward M. Carapezza, Proceedings of SPIE Vol. 5778 (SPIE, Bellingham, WA, 2005) · 0277-786X/05/$15 · doi: 10.1117/12.606574

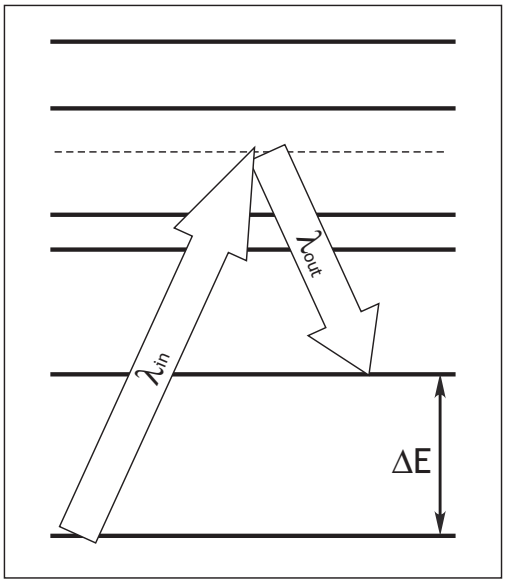

Figure 2. Schematic of a Stokes Raman transition.

We have developed a series of aperture codes for spectrometers that break this relationship between throughput and resolution, thus allowing the system designer to optimize each independently.[2] These aperture codes implement a form of multiplex measurement, and the resulting system is a computational optical sensor—the measurement is no longer isomorphic to the input signal. Instead, algorithmic methods must be employed to extract the spectrum from the measurement. By eliminating the requirement for isomorphism, the system can exist in regions of design space that were previously inaccessible. The result is an instrument that is significantly more flexible than traditional spectrometers.

In the context of remote chemical detection, this flexibility is primarily useful in allowing the size of the interrogation region to be controlled by operational requirements (*e.g.* can completely examine a target of size S in time T), rather than by optical requirements of throughput or spectral resolution. Consequently, instruments designed along these lines should prove significantly more useful in true operational environments.

This paper begins with a brief overview of Raman spectroscopy and its application in chemical detection. Next, we present a theoretical discussion of the performance trade-offs inherent in traditional spectrometers, and how the aperture coding eliminates these trade-offs to achieve exceptional performance for incoherent sources. Finally, we present experimental results from another spectroscopy project where we have incorporated this coding scheme.

2. RAMAN SPECTROSCOPY

Light scattered from atoms or molecules can be used to extract a vast amount of information about the scattering objects. The majority of the light scatters with the same energy that it had originally (when viewed in a inertial reference frame travelling with the scatterer). This light is said to be *elastically scattered* or *Rayleigh scattered*. When the spectrum of elastically scattered light is viewed from a reference frame *not* travelling with the scatterer, the light will be seen to have shifted in frequency as a result of the motion of the scatterer. This is known as the *Doppler shift* and can be used to extract information on the center-of-mass motion of an ensemble of scatterers as well as the temperature of the ensemble.

Even more valuable information can be gleaned from the small fraction of light (order 10^{-5}–10^{-9}) that changes energy upon scattering (again viewed in a reference frame travelling with the scatterer). This light is said to be *inelastically scattered* or *Raman scattered*.[3] The change in energy comes from energy exchange with the internal electronic, vibrational, and rotational states of the atoms or molecules. At typical temperatures, scatters will predominantly be in the internal ground state. As a result, the most common outcome is that the scattered light loses energy to the scatterer and emerges at a longer wavelength. This is known as the *Stokes component*. With high temperature, or otherwise energetically excited

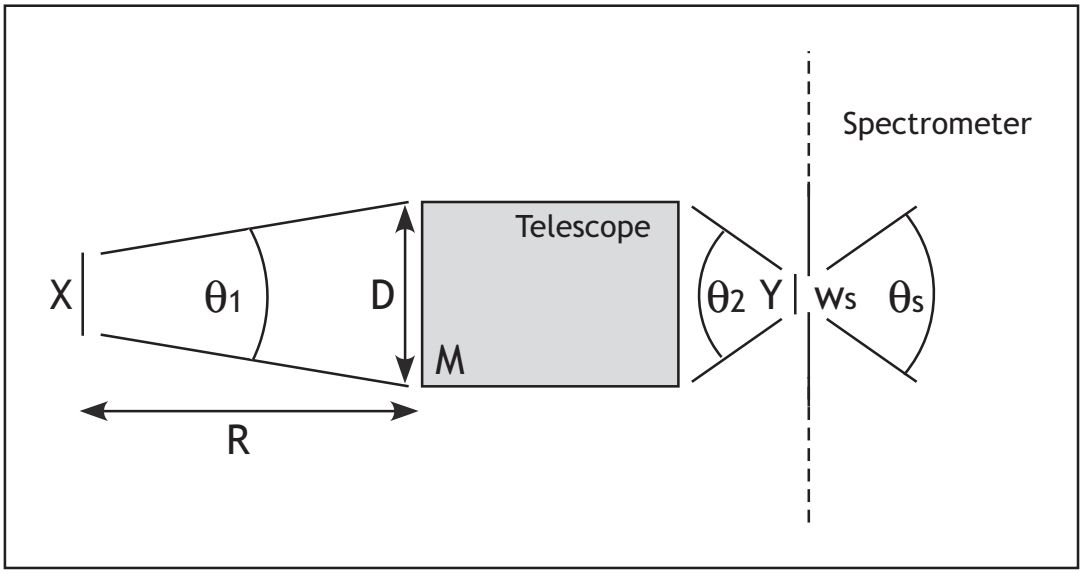

Figure 3. Optical parameter definition for an RRS.

scatters, the light can scatter with an increase of energy, and concomitant shorter wavelength. This is the *anti-Stokes component*. The change in the wavelength of the light (to either longer or shorter wavelength) is known as the *Raman shift*. A schematic of a Stokes Raman scattering event is shown in Fig. 2. The solid lines represent the ro-vibrational levels of the target molecule. The energy difference between the incoming and outgoing photons is given by the energy difference between the two internal states. Note that the incoming photon does not excite the molecule into a true excited state, but instead the transition acts as if there has been a transition through a virtual state (dashed line).

Measurement of the spectrum of Raman scattered light will reveal a number of Raman shifts. Each shift corresponds to a particular internal state transition of the scatterer. Because the energy levels of a molecule depends crucially on the composition of the molecule, the spectrum of Raman shifts is a highly specific "fingerprint" of the internal energy level structure. As such, it can be used for extremely precise chemical detection and identification.

3. TRADITIONAL OPTICAL SYSTEM

We consider a standard optical system for RRS, as shown in Fig. 3. A telescope of diameter D and overall angular magnification M is used to collect Raman photons produced in the interrogation region located at a range R. The interrogation spot is of diameter X. Although Raman emission is isotropic, the system collects only a small angular range $\Theta_1 \simeq D/R$. Given the magnification of the telescope system, the excitation spot is imaged to a spot of diameter $Y = X/M$ with angular spread $\Theta_2 = M\Theta_1$. The system is designed so that the image plane of the telescope is also the input plane of the spectrometer. The spectrometer has an input slit of width w_s and has an acceptance angle of Θ_s.

If no light is to be lost, the coupling between the telescope and spectrometer must obey

$$\Theta_2 \leq \Theta_s \tag{1}$$

and

$$Y \leq w_s. \tag{2}$$

Inserting the angular magnification relationship ($\Theta_2 = M\Theta_1$)into Eq. 1 yields

$$M\Theta_1 \leq \Theta_s. \tag{3}$$

Using the definition of the linear magnification ($Y = X/M$), we find

$$\frac{X\Theta_1}{Y} \leq \Theta_s. \tag{4}$$

If we then take $Y \simeq w_s$ to satisfy Eq. 2, this becomes

$$X\Theta_1 \lesssim w_s\Theta_s. \tag{5}$$

Which states the unsurprising (in hindsight) result that the optical invariant[4] of the spectrometer must equal or exceed the optical invariant of the source (again, although the Raman radiation is isotropic, we may neglect the angular components that are not captured by the telescope and treat it as having a limited angular spread).

We can cast Eq. 5 in a form more suited to system performance comparisons. The slit width of the spectrometer w_s is related to the spectrometer resolution through

$$w_s = \frac{d\Theta}{d\lambda} f\,\Delta\lambda. \tag{6}$$

Here, $d\Theta/d\lambda$ is the angular dispersion of the grating, f is the "throw" or "length" of the spectrometer, and $\Delta\lambda$ is the spectral resolution of the instrument. Similarly, we can write the acceptance angle of the spectrometer Θ_s in terms of the spectral bandwidth as

$$\Theta_s = \frac{d\Theta}{d\lambda}\,\Delta\Lambda. \tag{7}$$

Again, $d\Theta/d\lambda$ is the angular dispersion, and $\Delta\Lambda$ is the spectral bandwidth of the instrument.

Inserting Eqs. 6 and 7 into Eq. 5 and using the relationship $\Theta_1 \simeq D/R$, we can arrive at

$$\Delta\lambda \gtrsim \frac{XD}{\left(\frac{d\Theta}{d\lambda}\right)^2 f\,\Delta\Lambda\,R}. \tag{8}$$

To see the effect of this equation, we consider the following example. Ultraviolet (UV) radiation at 250 nm is used as a Raman excitation source*. The Raman fingerprint region of 500-3500 cm^{-1} then corresponds to a wavelength range of 253-273 nm. We assume the collection telescope has a diameter of 0.25 m (10 in.), and the spectrometer has a high dispersion grating with 3000 lines per millimeter (lpmm)†, and a throw of 0.25 m. We further assume that the spectrometer is a rather "fast" $f/3$. This means that the spectrometer has a fundamental spectral bandwidth of approximately 200 nm. The range to the interrogation region is 100 m. For an excitation spot size of 10 cm, the spectrometer must have a resolution no better than

$$\frac{(0.1)(0.25)}{(2.6\times10^{12})(0.25)(200\times10^{-9})(100)} \simeq 20\,\mathrm{nm}, \tag{9}$$

if all of the light captured by the telescope is to be used by the spectrometer. Note that the spectral region of interest, the Raman fingerprint region, is also 20 nm. Thus we are able to resolve no details in our region of interest! We see that to achieve even modest resolution over the spectral region of interest (for example, $\Delta\lambda \simeq 0.2\,\mathrm{nm}$) would require an interrogation region on the order of 1 mm.

Interrogation regions of this size are problematic for a variety of reasons. First, even moderate excitation powers in a region that small can result in damaging power density levels. Second, although reasonably-sized telescopes could in theory produce diffraction-limited spots that size and smaller, scattering during propagation is likely to produce spots that are much larger than the diffraction limit‡. Finally, with an extremely small interrogation region, it would take a very long time to cover a reasonably sized target of interest. Thus we see that, for a reasonable resolution to be achieved without sacrificing light throughput, we must abandon the slit-based design described above.

*The Raman scattering cross-section scales as $1/\lambda^4$, so UV excitation greatly enhances Raman photon generation. Further, solar emissions below about 290 nm are blocked by the ozone layer, dramatically reducing solar contributions to the background.

†For a grating arranged in a symmetric geometry, $(d\Theta/d\lambda)^2 \simeq 1/(4\kappa^2 - \lambda_0^2)$, where κ is the grating period and λ_0 is the center wavelength.

‡UV scatters strongly in the atmosphere. Additionally, many possible battlefield/security applications are likely to involve strongly scattering aerosols like smoke.

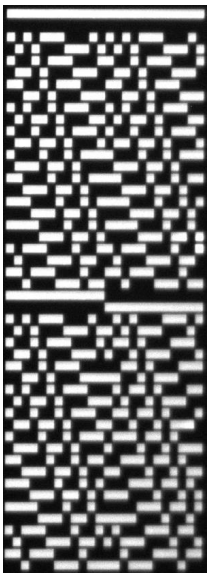

Figure 4. Microphotograph of an aperture mask (n=24).

4. APERTURE CODED OPTICAL SYSTEM

As mentioned previously, we have developed several classes of aperture-coded spectrometers that simultaneously maintain high spectral resolution and throughput for extended sources. These spectrometers are computational optical sensors, in that the output from the detector array is not recognizable as a spectrum, but must first be algorithmically processed.

Our designs involve replacing the input slit with a two-dimensional transmission pattern known as the *aperture code* or *aperture mask*. We have designs for several different classes of aperture codes. For the application considered here, the most useful is a pattern based on an order-n Hadamard matrix[§].[5] A mask based on an order-24 Hadamard matrix is shown in Fig. 4.

The salient attribute of these codes for the current discussion is that the spectral resolution depends on the size of individual *features* in the mask pattern, while the throughput depends on the *total* size of the pattern. Thus the resolution and throughput are decoupled in a manner that is impossible in the standard slit design.

If we designate the width of the mask features as w_m, then we can write the relationship to the spectral resolution in a form similar to Eq. 6

$$w_m = \frac{d\Theta}{d\lambda} f \, \Delta\lambda. \tag{10}$$

Continuing the example from above, we see that to achieve the 0.2 nm resolution that proved so problematic for the slit, we would need to use mask features on the order of

$$(1.6 \times 10^6)(0.25)(0.2 \times 10^{-9}) \simeq 80\,\mu\mathrm{m}. \tag{11}$$

Mask features of this size are completely feasible. In our research, we routinely use masks with features as small as 10 μm, without significant difficulty. Thus we could conceivably achieve resolutions as high as 0.02 nm on this spectrometer.

We now turn to the light throughput. Using the value calculated in Eq. 9 combined with Eq. 6, we can see that for the system we have considered, the image of the excitation source is approximately 8 mm in diameter. A 100×100 pattern of 80 μm features will cover this full area. Producing a Hadamard matrix of this complexity is not difficult.

[§]Hadamard matrices are the subset of square, unimodular, real matrices that have the maximal determinant for their size. The rows of a Hadamard matrix are mutually orthogonal, as are the columns. It can be shown mathematically that Hadamard matrices describe optimal multiplexing techniques in the presence of certain types of noise. It is conjectured that order-n Hadamard matrices exist for all n that are multiples of 4.

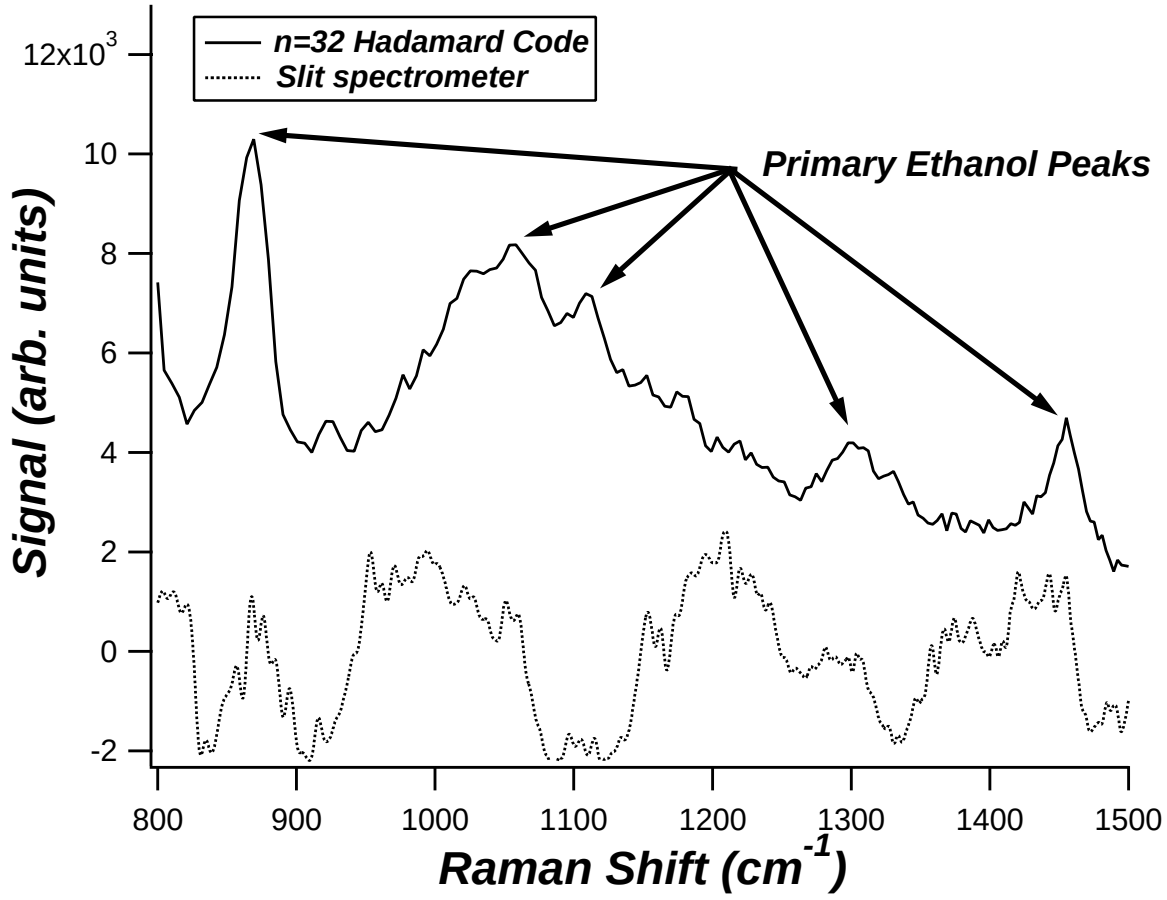

Figure 5. Performance of coded vs. non-coded spectrometers on a highly-incoherent source.

The mask-based approach inherently involves a 50% loss of light (half of the mask features are opaque). Therefore, comparison to the result in Eq. 9 is not strictly fair, as that case captured all of the light. However, stopping down the slit to 50% throughput would only improve the resolution by approximately a factor of 2 to 10 nm. Thus, even at equal throughput, the slit-based spectrometer has 50 times worse resolution than the simple coded aperture spectrometer we have considered in this section. Further, more complicated mask patterns do not decrease the throughput any further, but would continue to improve the spectral resolution of the coded aperture spectrometer. Finally, this performance is achievable at a fixed 50% throughput loss for arbitrarily large excitation spot sizes. As a result, the choice of excitation spot size can be based on operational requirements rather than the optical requirements imposed by the spectrometer.

5. EXPERIMENTAL VALIDATION OF THE CODING SCHEME

We have previously implemented this coding scheme in a Raman spectrometer designed for ethanol detection via *in vitro* analysis in blood or *in vivo* analysis in tissue. Raman detection of chemicals in biological materials has much in common with the remote chemical detection problem discussed in this paper.

First, both are highly scattering environments which limit the minimum size of the excitation region. As mentioned previously, for remote chemical detection, the scattering comes during the propagation to the target, either from atmospheric aerosols, or from the atmosphere itself. In the biological systems, the scattering arises primarily from the target—the dense, random arrangement of cells in blood or tissue. Regardless of the source, the scattering places a lower limit on the size of the interrogation region and produces a highly incoherent source.

Second, both are applications of Raman spectroscopy. As mentioned in Section 2, the cross-section for Raman scattering is extremely small. As a result, only a small fraction of the excitation photons actually produce a Raman photon and contribute to the signal. Thus signal strengths are extremely weak, and the throughput of any instrument is crucial. Similarly, the detection/identification problem in each requires that the instrument have a spectral resolution sufficient to recognize features corresponding to typical ro-vibrational transitions in the compounds of interest.

In our earlier experiments we were able to clearly detect the presence of a target molecule (ethanol) in a lipid/water solution that approximates the scattering properties of blood. A traditional slit spectrometer fails completely. Characteristic results are shown in Fig. 5. The solid curve is spectrum derived from our aperture coded instrument[¶]. All five primary ethanol peaks are visible. The dashed curve is the result from a high-performance benchtop spectrometer of conventional design. No clear signal is visible.

6. SUMMARY

Remote chemical detection is most easily accomplished by Raman spectroscopy. The source that results is highly incoherent—a source type which is a distinct challenge to traditional spectrometers. When working with incoherent sources, these spectrometers are forced into a trade-off between throughput and spectral resolution. Because the Raman signals generated by the remote chemicals are so weak, losing either throughput or resolution can be detrimental to the detection and identification process.

We have developed a multiplex spectrometer design that is optimized for working with incoherent sources. The spectral resolution and throughput of the instrument are not coupled and can be individually optimized in the system design. As a result, an RRS system built on this design can be significantly more sensitive and effective than designs based on traditional instruments. We have validated the coding schemes in other spectroscopy projects involving incoherent sources, are are now working towards constructing an RRS for remote chemical detection.

ACKNOWLEDGMENTS

This work was performed with the support of the National Institute on Alcoholism and Alcohol Abuse and the Defense Advanced Research Projects Agency (Microsystems Technology Office).

REFERENCES

1. J. P. Carrico, "Chemical-biological defense remote sensing: what's happening," in *Proc. SPIE Vol. 3383, Electro-Optical Technology for Remote Chemical Detection and Identification III*, pp. 45–56, Aug. 1998.
2. S. T. McCain, M. E. Gehm, Y. Wang., N. P. Pitsianis, and D. Brady, "Multiplex, multimodal spectrometry: Instrument design optimized for weak, diffuse sources." In progress, 2005.
3. J. R. Ferraro, K. Nakamoto, and C. W. Brown, *Introductory Raman Spectroscopy*, Academic Press, San Diego, 1994.
4. B. D. Guenther, *Modern Optics*, John Wiley, New York, 1989.
5. A. S. Hedayat, N. J. A. Sloane, and J. Stufken, *Orthogonal Arrays: Theory and Applications*, Springer Verlag, New York, 1999.

[¶]The specific aperture code was based on an order-32 Hadamard code